A New Viscoelastic Model for Preconditioning in Ligaments and Tendons

Ratchada Sopakayang

***Abstract*—In this paper, a new viscoelastic model is presented to describe the elastic and viscoelastic behaviors of ligaments and tendons during the preconditioning process. The model is formulated by accounting for the mechanical contribution of the main structures of ligaments and tendons, i. e., the collagen fibers, the proteoglycan-rich matrix and the coupling between the collagen fibers and the matrix. The coupling between the collagen fibers and the matrix is assumed to behave as the links binding the collagen fibers and the matrix together. According to the previous studies, the friction loss in ligaments and tendons plays a significant role on the stress softening and the decreasing of the hysteresis during preconditioning. Therefore, in this work, the links are assumed to gradually break during preconditioning and there will be no links breaking when the preconditioning is completed. Finally, the viscoelastic model can easily describe the stress softening and the decreasing of the hysteresis during preconditioning process. We believe that our model can provide a simple way to interpret the physical mechanism during the preconditioning process in ligaments and tendons.**

***Index Terms*—viscoelastic models, stress softening, preconditioning, ligaments, tendons.**

I. Introduction

LIGAMENTS and tendons are viscoelastic material in which the loading/stretching history has a great effect on the mechanical properties of the tissues. Therefore, before testing the soft biological specimens, the tissues need to experience the preconditioning process for canceling the loading/stretching history and setting up the same initial properties for all specimens. Preconditioning is a process that the successive cyclic loading/stretching is applied to the specimens until the mechanical properties of the specimens are unchanged. Preconditioning is usually be performed in two types of experiments; the load controlled and the displacement controlled. In the load controlled experiments, the maximum load of each successive cycle is fixed as a constant while in the displacement controlled experiments, the maximum displacement of each successive cycle is kept constant. As the previous studies, it is believed that the stress softening and the decreasing of hysteresis observed in the successive cycles during preconditioning are due to the structural changes occurring in the tissues [1].

Ligaments and tendons are usually preconditioned before performing mechanical testing, such as tensile, relaxation, creep and hysteresis tests. This preconditioning significantly influences their mechanical properties [2], [3], [4], [5], [6], [7], [8], [9], [10], [11]. In previous studies, [3] performed tensile tests of human quadriceps tendons and patellar ligaments before and after preconditioning. They found that the ultimate failure load and stiffness of these tissues were higher after preconditioning. In [2], Graf et al. performed relaxation experiments of primate patellar tendons before and after preconditioning and showed that the relaxation times were lower after preconditioning.

There is little known about the micro-structural changes occurring during preconditioning. In order to understand the mechanism of preconditioning, [12] compared the energy absorption (area in a hysteresis cycle) of the first and the last hysteresis cycle during preconditioning of normal canine anterior cruciate ligaments (ACLs) and treated canine ACLs in which the hyaluronic acid was enzymatically digested. They found that the energy absorption of the first hysteresis cycle of treated ACLs was much smaller than the energy absorption of the first hysteresis cycle of normal ACLs. The energy absorption was not significantly different for the last hysteresis cycle for both groups. Yahia and Drouin [12] suggested that the interfibrillar matrix containing water and other material such as proteoglycans and hyaluronic acid might be responsible for the observed hysteresis during preconditioning .

There have been several investigations which have explained the stress softening and energy dissipation during preconditioning [13], [14], [15], [16], [17]. In [13], Carew et al. tried to establish a protocol for preconditioning of porcine aortic valve cusps by using quasilinear viscoelastic (QLV) theory. Their simulation did not predict well the maximum stress of each cyclic loading due to the fact that the authors did not incorporate any structural mechanism into the model. Later, Nava et al. [15] introduced a phenomenological softening mechanism into a QLV model to describe preconditioning of bovine liver. Softening was assumed to be a function of the deformation history and a softening variable that changed over time. The model showed good prediction although the values of the model parameters were not presented by the authors. Both these phenomenological models did not help in understanding the mechanisms that govern preconditioning.

Currently, there is still no standard protocol used for preconditioning by experimental biomechanicians [18]. Therefore, developing mechanical models which can elucidate the role of the structural components of biological tissue during preconditioning could help in defining important standard parameters that can guide the design of the experiments. The main goal of this study is to present a viscoelastic model for parallel-fibered collageneous tissues which describes the viscoelastic behavior exhibited during preconditioning process.

II. Model Formulation

A. Basic Assumptions

The model is formulated by accounting for the mechanical contribution of the main structures of ligaments and tendons:

Manuscript received March 11, 2013; revised April 12, 2013.

R. Sopakayang is with the Department of Mechanical Engineering, Faculty of Engineering, Ubon Ratchathani University, Warinchumrap, Ubon Ratchathani, 34190 Thailand, e-mail: enratcso@ubu.ac.th.

ISBN: 978-988-19252-9-9
ISSN: 2078-0958 (Print); ISSN: 2078-0966 (Online)

the collagen fibers, the proteoglycan-rich matrix and the coupling between the collagen fibers and the matrix. The collagen fibers is modeled as multiple linear elastic springs arranged in parallel. Each spring which represents a collagen fiber has different wavinesses and therefore, is activated at different strains. The elastic modulus of each straight fiber is defined as E_f. The proteogycan-rich matrix surrounded collagen fibers is modeled as a Maxwell element which is a series of an elastic spring with an elastic modulus E_m and a viscous dashpot with a coefficient of viscosity η_m. The multiple elastic springs which represent the collagen fibers and the Maxwell element which represents the matrix are then connected in parallel. The links binding the collagen fibers and the matrix together are modeled as two identical groups of the parallel arrangement of numerous elastic springs with an elastic modulus E_c. The strain of the first group of the elastic springs is assumed to be the same with the strain of the elastic springs representing the collagen fibers while the strain of the second group of the elastic springs is assumed to be the same with the strain of the elastic spring representing the elastic component of the matrix. These two groups of elastic springs are assumed to gradually break simultaneously during preconditioning which contributes the stress softening and the decreasing of the hysteresis in preconditioning process. The schematic of the proposed model described is shown in Fig. 1.

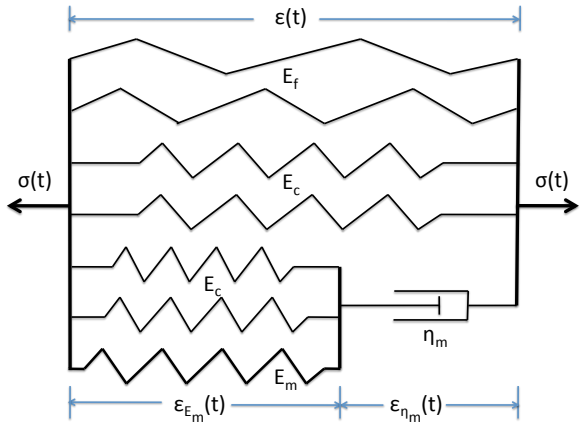

Fig. 1. Schematic of Viscoelastic Model.

B. Modeling Framework

The total stress of the tissue, $\sigma(t)$, where t denotes the time, is given by

$$\sigma(t) = \sigma_f(t) + \sigma_{c,f}(t) + \sigma_{c,m}(t) + \sigma_m(t)\,, \tag{1}$$

where $\sigma_f(t)$ is the stress of the collagen fibers. $\sigma_{c,f}(t)$ and $\sigma_{c,m}(t)$ are the stresses of the links between the collagen fibers and the matrix which associate to the collagen fibers and the matrix, respectively. $\sigma_m(t)$ is the stress of the matrix.

Due to the arrangement of the elastic springs of the links which associate to the matrix, the elastic spring of the matrix and the viscous dashpot of the matrix, one has that

$$\sigma_{c,m}(t) + \sigma_m(t) = \sigma_\eta(t)\,, \tag{2}$$

where $\sigma_\eta(t)$ is the stress of the viscous component of the matrix.

Moreover, the total strain of the tissue, $\varepsilon(t)$, is

$$\varepsilon(t) = \varepsilon_f(t) = \varepsilon_{c,f}(t) = \varepsilon_{c,m}(t) + \varepsilon_\eta(t)\,, \tag{3}$$

where $\varepsilon_{c,m}(t) = \varepsilon_m(t)$. $\varepsilon_f(t)$ is the strain of the fibers. $\varepsilon_{c,f}(t)$ and $\varepsilon_{c,m}(t)$ are the strains of the links between the fibers and the matrix which associate to the fibers and the matrix, respectively. Moreover, $\varepsilon_m(t)$ and $\varepsilon_\eta(t)$ are the strains of the elastic and viscous components of the matrix, respectively.

The stress of the fibrous component of the tissue, $\sigma_f(t)$, is defined by using a structural approach as previously done by other investigators [19], [20]. The collagen fibers are assumed to become straight at different strains, $\varepsilon_s \geq 0$, defined by the following exponential probability density function

$$p(\varepsilon_s) = \alpha e^{-\alpha\varepsilon_s} \quad \text{with} \quad \int_0^\infty p(\varepsilon_s)d\varepsilon_s = 1\,, \tag{4}$$

where $\alpha > 0$ denotes the so-called rate parameter and, for $\varepsilon_s \geq 0$, $P(\varepsilon)$ denotes the exponential cumulative distribution function defined as

$$P(\varepsilon) = \int_0^\varepsilon p(\varepsilon_s)d\varepsilon_s = 1 - e^{-\alpha\varepsilon}\,. \tag{5}$$

The stress of collagen fibers is given for $\varepsilon \geq \varepsilon_s$ by

$$\sigma_f(t) = \int_0^{\varepsilon(t)} E_f(\varepsilon(t) - \varepsilon_s)p(\varepsilon_s)d\varepsilon_s\,, \tag{6}$$

where E_f denotes the elastic modulus of each straight collagen fiber.

The total stress of links between the collagen fibers and the proteoglycan-rich matrix is defined as $\sigma_c(t)$ and is assumed to be a contribution of two structural components. The first structural component is the contact surface between the links and the fibers which contributes the stress of the links associating to the fibers, $\sigma_{c,f}(t)$ while the second structural component is the contact surface between the links and the matrix which contributes the stress of the links associating to the matrix, $\sigma_{c,m}(t)$. Therefore, the total stress of the links between the fibers and the matrix is given by

$$\sigma_c(t) = \sigma_{c,f}(t) + \sigma_{m,f}(t)\,, \tag{7}$$

The stress determined by the links between the collagen fiber and the proteoglycan-rich matrix is defined by using an approach similar to the one presented by Raischel et al. [21] and De Tommasi et al. [22] for different materials. The links are assumed to break when their strains, $\varepsilon_{c,f}$ and $\varepsilon_{c,m}$, reach some values $\varepsilon_b \geq 0$ that are defined by an exponential probability density function. Specifically, the stress of the links associating to the fibers is given by

$$\sigma_{c,f}(t) = E_c\varepsilon_{c,f}(t)(1 - P(\varepsilon_{c,f}(t))) + E_c\int_0^{\varepsilon_{c,f}(t)} \varepsilon_b p(\varepsilon_b)d\varepsilon_b\,, \tag{8}$$

ISBN: 978-988-19252-9-9
ISSN: 2078-0958 (Print); ISSN: 2078-0966 (Online)

and the stress of the links associating to the matrix is given by

$$\sigma_{c,m}(t) = E_c\varepsilon_{c,m}(t)(1 - P(\varepsilon_{c,m}(t))) + E_c\int_0^{\varepsilon_{c,m}(t)} \varepsilon_b p(\varepsilon_b)d\varepsilon_b\,, \quad (9)$$

where E_c is the elastic constant of the links.

In Eq. 8 and Eq. 9, $p(\varepsilon_b)$ is the probability density function of an exponential distribution defined, for $\varepsilon_b \geq 0$, as

$$p(\varepsilon_b) = \beta e^{-\beta\varepsilon_b}\,, \quad (10)$$

where $\beta > 0$ denotes the so-called rate parameter. The exponential cumulative distribution function of the links associating to the fibers, $P(\varepsilon_{c,f})$, and the matrix, $P(\varepsilon_{c,m})$ can be written as follows.

$$P(\varepsilon_{c,f}) = \int_0^{\varepsilon_{c,f}} p(\varepsilon_b)d\varepsilon_b = 1 - e^{-\beta\varepsilon_{c,f}}\,. \quad (11)$$

$$P(\varepsilon_{c,m}) = \int_0^{\varepsilon_{c,m}} p(\varepsilon_b)d\varepsilon_b = 1 - e^{-\beta\varepsilon_{c,m}}\,. \quad (12)$$

The first term on the right-hand side of Eq. 8 and Eq. 9 are the stresses of all the unbroken links while the second term are the stresses of all the broken links. These stresses of the broken links are not transferred to the unbroken links.

The stress of the elastic component of the matrix is defined as

$$\sigma_m(t) = E_m\varepsilon_m(t)\,, \quad (13)$$

where E_m denotes the elastic modulus of the matrix.

The stress of the viscous component of the matrix is defined as

$$\sigma_\eta(t) = \eta_m\varepsilon'_\eta(t)\,, \quad (14)$$

where η_m denotes the viscous modulus of the matrix and a prime denotes the differentiation with respect to t.

After noting that $\sigma_{c,m}(t) + \sigma_m(t) = \sigma_\eta(t)$ from Eq. 2, $\sigma_\eta(t) = \eta_m\varepsilon'_\eta(t)$ from Eq. 14 and that $\sigma(t) = \sigma_f(t) + \sigma_{c,f}(t) + \sigma_{c,m}(t) + \sigma_\eta(t)$ from Eq. 1, Eq. 1 can be rewritten as

$$\sigma(t) = \sigma_f(t) + \sigma_{c,f}(t) + \eta_m\varepsilon'_\eta(t)\,. \quad (15)$$

Moreover, since $\varepsilon_\eta(t) = \varepsilon(t) - \varepsilon_{c,m}(t)$ from Eq. 3, Eq. 15 becomes

$$\sigma(t) = \sigma_f(t) + \sigma_{c,f}(t) + \eta_m(\varepsilon'(t) - \varepsilon'_{c,m}(t))\,. \quad (16)$$

By recalling that $\sigma_{c,m}(t) = E_c\varepsilon_{c,m}(t)(1 - P(\varepsilon_{c,m}(t))) + E_c\int_0^{\varepsilon_{c,m}(t)} \varepsilon_b p(\varepsilon_b)d\varepsilon_b$ from Eq. 9, $\sigma_m(t) = E_m\varepsilon_m(t)$ from Eq. 13, $\sigma_\eta(t) = \eta_m\varepsilon'_\eta(t)$ from Eq. 14 and that $\sigma_{c,m}(t) + \sigma_m(t) = \sigma_\eta(t)$ from Eq. 2, Eq. 2 can be rewritten as

$$E_c\varepsilon_{c,m}(t)(1 - P(\varepsilon_{c,m}(t))) + E_c\int_0^{\varepsilon_{c,m}(t)} \varepsilon_b p(\varepsilon_b)d\varepsilon_b + E_m\varepsilon_m(t) = \eta_m\varepsilon'_\eta(t)\,. \quad (17)$$

Moreover, since $\varepsilon_{c,m}(t) = \varepsilon_m(t)$ and $\varepsilon_\eta(t) = \varepsilon(t) - \varepsilon_{c,m}(t)$ from Eq. 3, Eq. 17 can be rearranged and rewritten as

$$\varepsilon'_{c,m}(t) = \varepsilon'(t) - \frac{E_c}{\eta_m}\varepsilon_{c,m}(t)(1 - P(\varepsilon_{c,m}(t))) - \frac{E_c}{\eta_m}\int_0^{\varepsilon_{c,m}(t)} \varepsilon_b p(\varepsilon_b)d\varepsilon_b - \frac{E_m}{\eta_m}\varepsilon_{c,m}(t)\,. \quad (18)$$

By recalling $p(\varepsilon_b) = \beta e^{-\beta\varepsilon_b}$ and $P(\varepsilon_{c,m}) = 1 - e^{-\beta\varepsilon_{c,m}}$ from Eqs. 10 and 12, respectively, Eq. 18 becomes

$$\varepsilon'_{c,m}(t) = \varepsilon'(t) + \frac{E_c}{\beta\eta_m}(e^{-\beta\varepsilon_{c,m}(t)} - 1) - \frac{E_m}{\eta_m}\varepsilon_{c,m}(t)\,. \quad (19)$$

By recalling that $\sigma_f(t) = \int_0^{\varepsilon(t)} E_f(\varepsilon(t) - \varepsilon_s)p(\varepsilon_s)d\varepsilon_s$ from Eq. 6 and $\sigma_{c,f}(t) = E_c\varepsilon_{c,f}(t)(1 - P(\varepsilon_{c,f}(t))) + E_c\int_0^{\varepsilon_{c,f}(t)} \varepsilon_b p(\varepsilon_b)d\varepsilon_b$ from Eq. 8 and $\varepsilon(t) = \varepsilon_{c,f}(t)$ from Eq. 3, Eq. 16 becomes

$$\sigma(t) = \int_0^{\varepsilon(t)} E_f(\varepsilon(t) - \varepsilon_s)p(\varepsilon_s)d\varepsilon_s + E_c\varepsilon(t)(1 - P(\varepsilon_{c,f}(t))) + E_c\int_0^{\varepsilon(t)} \varepsilon_b p(\varepsilon_b)d\varepsilon_b + \eta_m(\varepsilon'(t) - \varepsilon'_{c,m}(t))\,. \quad (20)$$

By substituting Eq. 19 into Eq. 20, Eq. 20 can be rewritten as

$$\sigma(t) = \int_0^{\varepsilon(t)} E_f(\varepsilon(t) - \varepsilon_s)p(\varepsilon_s)d\varepsilon_s + E_c\varepsilon(t)(1 - P(\varepsilon_{c,f}(t))) + E_c\int_0^{\varepsilon(t)} \varepsilon_b p(\varepsilon_b)d\varepsilon_b + (E_m\varepsilon_{c,m}(t) - \frac{E_c}{\beta}(e^{-\beta\varepsilon_{c,m}} - 1))\,. \quad (21)$$

After differentiating both sides of Eq. 21 with respect to t, one obtains that

$$\sigma'(t) = \frac{d}{dt}[\int_0^{\varepsilon(t)} E_f(\varepsilon(t) - \varepsilon_s)p(\varepsilon_s)d\varepsilon_s] + E_c\frac{d}{dt}[\varepsilon(t)(1 - P(\varepsilon_{c,f}(t)))] + E_c\frac{d}{dt}[\int_0^{\varepsilon(t)} \varepsilon_b p(\varepsilon_b)d\varepsilon_b))] + \frac{d}{dt}[E_m\varepsilon_{c,m}(t) - \frac{E_c}{\beta}(e^{-\beta\varepsilon_{c,m}} - 1)]\,. \quad (22)$$

Firstly, by applying Leibniz's rule for differentiation of an integral to Eq. 22 one obtains that

$$\frac{d}{dt}[\int_0^{\varepsilon(t)} E_f(\varepsilon(t) - \varepsilon_s)p(\varepsilon_s)d\varepsilon_s] = E_f\varepsilon'(t)\int_0^{\varepsilon} p(\varepsilon_s)d\varepsilon_s\,. \quad (23)$$

It must be noted that for $p(\varepsilon_s)$ defined by Eq. 4, $\int_0^{\varepsilon} p(\varepsilon_s)d\varepsilon_s = 1 - e^{-\alpha\varepsilon}$, which is the exponential cumulative density function. Thus, Eq. 23 can be written as

$$\frac{d}{dt}[\int_0^{\varepsilon(t)} E_f(\varepsilon(t) - \varepsilon_s)p(\varepsilon_s)d\varepsilon_s] = E_f\varepsilon'(t)\left(1 - e^{-\alpha\varepsilon}\right)\,. \quad (24)$$

ISBN: 978-988-19252-9-9
ISSN: 2078-0958 (Print); ISSN: 2078-0966 (Online)

Secondly, by recalling $P(\varepsilon_{c,f}) = 1 - e^{-\beta\varepsilon_{c,f}}$ and $\varepsilon(t) = \varepsilon_{c,f}(t)$ from Eq. 11 and Eq. 3, respectively, the second term of Eq. 22 can be rewritten as

$$E_c \frac{d}{dt}[\varepsilon(t)(1 - P(\varepsilon(t)))] = E_c \frac{d}{dt}[\varepsilon e^{-\beta\varepsilon}] = E_c \varepsilon'(t) e^{-\beta\varepsilon}(1 - \beta\varepsilon)\,. \quad (25)$$

Thirdly, by applying Leibniz's rule for differentiation of an integral to Eq. 22 one obtains that

$$\frac{d}{dt}[\int_0^{\varepsilon(t)} \varepsilon_b p(\varepsilon_b) d\varepsilon_b] = \varepsilon(t) p(\varepsilon) \varepsilon'(t)\,. \quad (26)$$

It must be noted that for $p(\varepsilon_b) = \beta e^{-\beta\varepsilon_b}$ defined by Eq. 10, p$(\varepsilon(t)) = \beta e^{-\beta\varepsilon(t)}$, which is the exponential probability distribution function. Thus, Eq. 26 can be written as

$$\frac{d}{dt}[\int_0^{\varepsilon(t)} \varepsilon_b p(\varepsilon_b) d\varepsilon_b] = \beta\varepsilon(t) e^{-\beta\varepsilon} \varepsilon'(t)\,. \quad (27)$$

By using Eq. 24, Eq. 25 and Eq. 27, Eq. 22 can be rewritten as

$$\sigma'(t) = E_f \varepsilon'(t)(1 - e^{-\alpha\varepsilon}) + E_c \varepsilon'(t) e^{-\beta\varepsilon(t)} + \varepsilon'_{c,m}(t)(E_m + \beta E_c e^{-\beta\varepsilon_{c,m}(t)})\,. \quad (28)$$

Eqs. 19 and 28 form a system of ordinary differential equations that can be solved numerically to find $\varepsilon_{c,m}(t)$ and $\sigma(t)$ after assigning the initial conditions.

In order to describe the stress-strain relationship of each cyclic loading in preconditioning by solving numerically the system of ordinary differential equations, Eqs. 19 and 28, the cyclic strain history of the tissue, $\varepsilon(t)$, is assumed to have the form

$$\varepsilon(t) = \begin{cases} bt - (2i-2)bt_0 & \text{for } (2i-2)t_0 \le t < (2i-1)t_0, \\ -bt + (2i)bt_0 & \text{for } (2i-1)t_0 \le t < (2i)t_0, \end{cases} \quad (29)$$

where b and t_0 are constants, i is a positive integer that denotes the number of loading cycles.

C. Softening Model

The stress-strain relationships for all the cycles that follow the 1^{st} cycle can be computed by accounting for the decreasing of the elastic modulus of the links between the collagen fibers and the matrix, E_c, by using the softening model, Eq. 30, which can be written as

$$E_c^{i+1} = E_c^1 e^{-(i-1)}\,. \quad (30)$$

where E_c^1 and E_c^{i+1} denote the E_c for the 1^{st} cycle and the $(i+1)^{th}$ cycle, respectively.

III. Results

The preconditioning process is simulated by applying the strain history, Eq. 29, and the softening model, Eq. 29, to the ordinary differential equation system, Eq. 19 and Eq. 28, therefore the stress strain relationships for all cycles can be presented. In this study, the preconditioning is simulated by assuming the parameters that $\varepsilon' = 0.2/s$, $\varepsilon_M = 0.04$, $t_0 = 0.2s$, $E_f = 500$ MPa, $E_m = 1$ MPa, $\eta = 1MPa.s$, $\alpha = 10$, $\beta = 0.01$ and $E_c^1 = 10$ MPa. The stress-strain curves for the 1^{st} cycle are shown in Fig. 2 while the stress-strain curves of the 1^{st} and the 2^{nd} cycles are shown in Fig. 3.

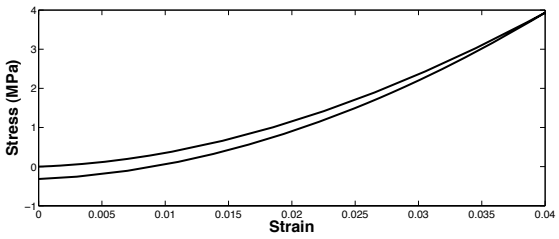

Fig. 2. Preconditioning simulation for the 1^{st} cycle.

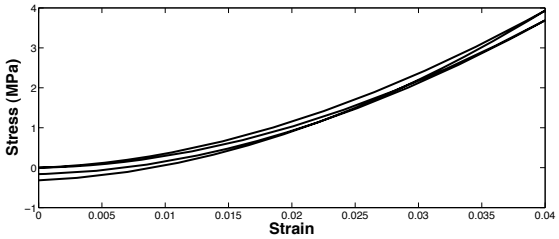

Fig. 3. Preconditioning simulation for the 1^{st} and 2^{nd} cycles.

In this study, it has been calculated that the stress-strain curves of preconditioning remain constant since the 6^{th} cycle, therefore the preconditioning is simulated and shown in Fig. 4. for 7 cycles. The decreasing of the maximum stress in each cycle during the preconditioning is shown in Fig. 5. In this simulation case, it is observed that the maximum stress of the first hysteresis cycle is 3.96 MPa and it remains constant as 3.55 MPa since the 6^{th} cycle.

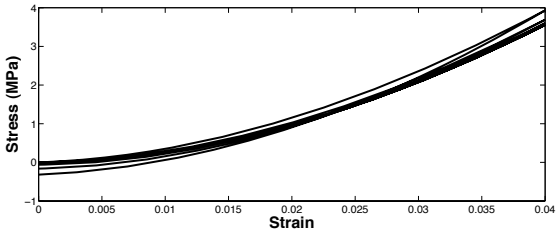

Fig. 4. Preconditioning simulation for 7 cycles.

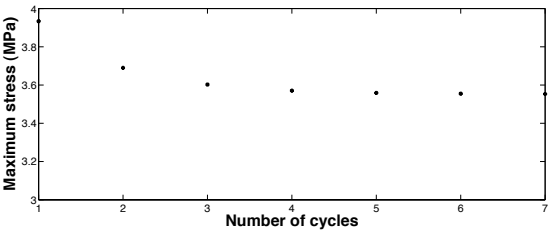

Fig. 5. The decreasing of the maximum stress in each cycle during the preconditioning process.

The stress softening and the decreasing of hysteresis is influenced from the breaking of the links between the fibers and the matrix during preconditioning. Therefore, the elastic

ISBN: 978-988-19252-9-9
ISSN: 2078-0958 (Print); ISSN: 2078-0966 (Online)

modulus of the links is assumed to be exponentially decreased until it goes to zero as shown in Fig. 6.

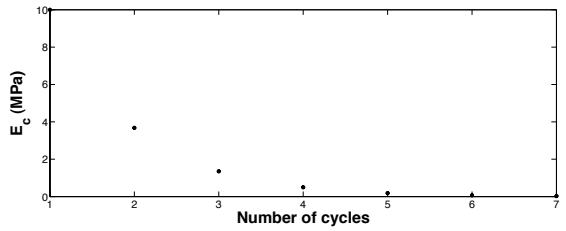

Fig. 6. The decreasing of E_c in each cycle during the preconditioning process.

IV. Discussion and Conclusions

A new viscoelastic model, for which the schematic is shown in Fig. 1, is presented to describe the viscoelastic behavior exhibited during preconditioning process. This viscoelastic model is formulated by accounting for the mechanical contributions of the collagen fibers, the intervening proteoglycan-rich matrix and the coupling between the collagen fibers and the matrix. The coupling between the collagen fibers and the matrix is assumed to behave as the links binding the collagen fibers and the matrix together. It is believed that the stress softening and the decreasing of hysteresis (energy dissipation) during preconditioning occur due to the friction loss and the changes of the internal structure of the tissues [1]. It has been experimentally observed that the maximum stresses and hysteresis of successive stress-strain cycles gradually decrease during preconditioning and they finally remain unchanged when the tissues are completely preconditioned [1], [7]. Therefore, in this study, the links between the collagen fibers and the matrix are assumed to progressively fail while the collagen fibers are assumed to gradually become active under the loading paths of all cycles. For the unloading paths, the collagen fibers and the unbroken links are assumed to gradually move back to their original positions while the broken links occurred during the loading paths are not transferred to the unbroken links. Because of the decreasing of the amount of the broken links occurred in successive cycles, in the softening model (Eq. 30), the elastic modulus of the links which associates to amounts of the broken links between the collagen fibers and the matrix is assumed to exponentially decreases when the number of cycle increases.

Because of the lack of some information from the experiment in the paper [7], the exact quantitative simulation can be done by requiring a specific experimental data of preconditioning. The parameters in the proposed model are directly related to the physiology of the internal structure of ligaments and tendons during preconditioning. In general, they can be found by validating the model with some experimental data which can be carried out in future works. For this work, in order to describe the viscoelastic behavior during preconditioning process, the parameters in the model are assumed as $E_f = 500$ MPa, $E_m = 1$ MPa, $\eta = 1MPa.s$, $\alpha = 10$, $\beta = 0.01$ and $E_c^1 = 10$ MPa while the constants in the cyclic strain history are assumed as $\varepsilon' = 0.2/s$, $\varepsilon_M = 0.04$ and $t_0 = 0.2s$. The values of these parameters are estimated based on the values of the parameters in a similar model presented in a previous work [23].

The results of the model simulations are shown in Fig. 2 - Fig. 4. The preconditioning simulation for the 1^{st} cycle is presented in Fig. 2. which is observed that the model could capture the nonlinearities of the loading and unloading stress-strain curves, and the hysteresis (energy dissipation) during the cyclic loading. According to the model, the nonlinearities are due to the parameters, α and β, which indicate the rate of the amount of the active fibers and the rate of the amount of broken links between the fibers and the matrix, respectively. The hysteresis is due to the broken links occurred in the loading path of the cyclic loading which is indicated by the parameter, β, and the viscoelastic property of the matrix which is specified by the parameters, E_m and η, which represent the elastic modulus and the viscosity of the matrix, respectively. The preconditioning simulation for the 1^{st} and 2^{nd} cycles is shown in Fig. 3. It is observed that the maximum stress and the hysteresis of the 1^{st} cycle are greater than the maximum stress and the hysteresis of the 2^{nd} cycle, respectively. The model parameter that captures these behaviors is the E_c which exponentially decreases when the number of cyclic loading increases. E_c indicates the value of the modulus stiffness of the links between the collagen fibers and the matrix. Because of the breakage of the links in every loading cycle, E_c is assumed to decrease in successive cycles as the softening model presented in Eq. 30. Therefore, the softening model could capture both the stress softening and the decreasing of the hysteresis in successive cycles during preconditioning. Fig. 4. shows the preconditioning simulation for 7 stress-strain cycles. It could be noticed that the stress-strain curves remain unchanged since the 6^{th} cycle which could be interpreted that the coupling between the collagen fibers and the matrix would not play the role on the structural changes during preconditioning since the 6^{th} cycle of the cyclic loading. Therefore, the maximum stress of each cycle would exponentially decrease until the 6^{th} cycle and remain unchanged in successive cycles as shown in Fig. 5. In the same way, the stiffness of the links, E_c, of each cycle exponentially decreases and becomes zero since the 6^{th} cycle as shown in Fig. 6. which means the mechanical contribution of the links or the coupling between the collagen fibers and the matrix does not influence the viscoelastic properties of the tissues after the 6^{th} cycle. At this stage, it could be stated that the tissues are completely preconditioned.

In conclusion, a new modeling framework is presented for describing the mechanical response of ligaments and tendons exhibited during preconditioning process. The model simulation seems to have excellent qualitative agreement with the experimental data of Dorow [7]. The proposed model here could be extended to describe other viscoelastic phenomena in ligaments and tendons, such as creep and relaxation. Moreover, it could be also applied to describe the viscoelasticity of other collagenous tissues. More importantly, it could be employed to illustrate the role of the mechanical response of the coupling between the collagen fibers and the matrix in collagenous tissues. According to the model simulations in this study, it could be suggested that the energy dissipation during preconditioning might due to the effect of the structural changes in the coupling between the collagen fibers and the matrix which associate to the friction

ISBN: 978-988-19252-9-9
ISSN: 2078-0958 (Print); ISSN: 2078-0966 (Online)

loss or the disconnection of some contact surfaces between the collagen fibers and the matrix. However, based on the excellent qualitative agreement and the adjustable parameters in the model, the quantitative agreement could be done in the future experimental and theoretical studies.

REFERENCES

[1] Y. C. Fung, *Biomechanics: Mechanical properties of living tissues*, 2nd ed. New York: Springer-Verlag, 1993.
[2] K. Graf, B., J. Vanderby, R., J. Ulm, M., P. Rogalski, R., and J. Thielke, R., "Effect of preconditioning on the viscoelastic response of primate patellar tendon," *The Journal of Arthroscopic and Related Surgery*, vol. 10, pp. 90–96, 1994.
[3] L. Schatzmann, P. Brunner, and H. U. Staubli, "Effect of cyclic preconditioning on the tensile properties of human quadriceps tendons and patellar ligaments," *Knee Surgery Sports Traumatology Arthroscopy*, vol. 6, pp. 56–61, 1998.
[4] U. Staubli, H., L. Schatzmann, P. Brunner, L. Rincon, and L. P. Nolte, "Mechnical tensile properties of the quadriceps tendon and patellar ligament in young adults," *The American Journal of Sports Medicine*, vol. 27, pp. 27–34, 1999.
[5] J. R. Funk, G. W. Hall, J. R. Crandall, and W. D. Pilkey, "Linear and quasi-linear viscoelastic characterization of ankle ligaments," *Journal of Biomechanical Engineering*, vol. 122, pp. 15–21, 2000.
[6] J. A. Weiss and J. C. Gardiner, "Computational modeling of ligament mechanics," *Critical Reviews in Biomedical Engineering*, vol. 29, pp. 1–70, 2001.
[7] C. Dorow, N. Krstin, and F. G. Sander, "Experiments to determine the material properties of the periodontal ligaments," *Journal of Orofacial Orthopedics*, vol. 63, pp. 94–104, 2002.
[8] F. Genna, L. Annovazzi, C. Bonesi, P. Fogazzi, and C. Paganelli, "On the experimental determination of some mechanical properties of porcine periodontal ligament," *Meccanica*, vol. 43, pp. 55–73, 2008.
[9] T. Cheng and R. Z. Gan, "Mechanical properties of anterior malleolar ligament from experimental measurement and material modeling analysis," *Biomechanics and Modeling in Mechanobiology*, vol. 7, pp. 387–394, 2008.
[10] A. Teramoto and Z. P. Luo, "Temporary tendon strengthening by preconditioning," *Clinical Biomechanics*, vol. 23, pp. 619–622, 2008.
[11] A. Teramoto, W. R. Su, and Z. P. Luo, "Effect of cyclic preconditioning on the failure load, strength and stiffness of multiple rat tendons and ligaments," *Journal of Musculoskeletal Research*, vol. 11, pp. 89–95, 2008.
[12] L. H. Yahia and G. Drouin, "Study of the hysteresis phenomenon on canine anterior cruciate ligaments," *Journal of Biomedical Engineering*, vol. 12, pp. 57–61, 1990.
[13] E. O. Carew, J. E. Barber, and I. Vesely, "Role of preconditioning and recovery time in repeated testing of aortic valve tissues: Validation through quasilinear viscoelastic theory," *Annals of Biomedical Engineering*, vol. 28, pp. 1093–1100, 2000.
[14] A. Sverdlik and Y. Lanir, "Time-dependent mechanical behavior of sheep digital tendons, including the effects of preconditioning," *Transaction of the American Society of Mechanical Engineers: Journal of Biomechanical Engineering*, vol. 124, pp. 78–84, 2002.
[15] A. Nava, E. Mazza, O. Haefner, and M. Bajka, "Experimental observation and modeling of preconditioning in soft biological tissues," *Lecture Notes in Computer Science*, vol. 3078, pp. 1–8, 2004.
[16] P. Ciarletta, P. Dario, and S. Micera, "Pseudo - hyperelastic model of tendon hysteresis from adaptive recruitment of collagen type i fibrils," *Biomaterials*, vol. 29, pp. 764–770, 2008.
[17] O. Lokshin and Y. Lanir, "Viscoelasticity and preconditioning of rat skin under uniaxial stretch: Microstructural constitutive characterization," *Transaction of the American Society of Mechanical Engineers: Journal of Biomechanical Engineering*, vol. 131, pp. 1–10, 2009.
[18] N. Conza, "Engineering issues in experimental biomedicine series. part 3: Tissue preconditioning," *Experimental Techniques*, vol. 29, pp. 43–46, 2005.
[19] Y. Lanir, "A structural theory for the homogeneous biaxial stress-strain relationship in flat collageneous tissues," *Journal of Biomechanics*, vol. 12, pp. 423–436, 1979.
[20] R. De Vita and W. S. Slaughter, "A structural constitutive model for the strain rate-dependent behavior of anterior cruciate ligaments," *International Journal of Solids and Structures*, vol. 43, pp. 1561–1570, 2006.
[21] F. Raischel, F. Kun, and H. Herrmann, "Failure process of a bundle of plastic fibers," *Physical Review E*, vol. 73, p. 66101, 2006.
[22] D. De Tommasi, G. Puglisi, and G. Saccomandi, "A micromechanics-based model for the mullins effect," *Journal of Rheology*, vol. 50, p. 495, 2006.
[23] R. Sopakayang and R. De Vita, "A mathematical model for creep, relaxation and strain stiffening in parallel-fibered collagenous tissues," *Medical Engineering Physics*, vol. 33, pp. 1056–1063, 2011.

ISBN: 978-988-19252-9-9
ISSN: 2078-0958 (Print); ISSN: 2078-0966 (Online)